Appl Phys A (2010) 100: 223–230
DOI 10.1007/s00339-010-5579-2

Applied Physics A
Materials Science & Processing

Nonlinear optical properties of nanometer-size silver composite azobenzene containing polydiacetylene film

Xin Chen · Jun Tao · Gang Zou · Qijin Zhang · Pei Wang

Received: 28 August 2009 / Accepted: 22 January 2010 / Published online: 9 February 2010

Abstract Diacetylene monomer containing p-nitrophenyl azobenzene moiety (NADA) was synthesized. Silver nanoparticles with different concentrations were adulterated in the above polymerized NADA (PNADA) films and the third-order nonlinear optical properties were investigated in detail. UV–vis spectra and transmission electron microscopy were used to confirm the formation of PNADA/Ag nanocomposite films. The silver nanoparticles (average size of 10 nm) were well dispersed in the polymer films. The value of the nonlinear refractive index n_2 for PNADA films (8.48×10^{-15} cm^2/W) was much higher than that of pure polydiacetylene films. Further, the introduction of silver nanoparticles into the PNADA polymer films led to the further enhancement of nonlinear optical properties. The maximum value of n_2 for PNADA/Ag nanocomposite films could be 11.6×10^{-15} cm^2/W. This enhancement should be ascribed to the surface plasmon resonance of silver nanoparticles.

1 Introduction

Nonlinear optical (NLO) materials are required for high-speed optical network systems dealing with a large amount of data. In particular, organic third-order NLO materials, such as π-conjugated polymers, are powerful candidates for developing photonics devices, due to the high-speed NLO response and easy chemical modification in comparison with inorganic systems [1]. Among these π-conjugated organic NLO materials, polydiacetylene (PDA) possesses excellent third-order NLO response properties in the range of femtoseconds to sub-picoseconds, which is attributed to delocalized π-conjugated electrons along the main chain backbone [2–7]. However, the magnitude of the effective third-order NLO susceptibility Re $\chi^{(3)}$ for PDA is still not sufficient for device applications. Many theoretical and experimental efforts had been made to improve the effective third-order NLO susceptibility Re $\chi^{(3)}$ of the PDA system [8–13]. Consequently, the syntheses and optoelectronic properties of PDA derivatives had been extensively studied, especially the π-conjugation extended between main chain and side chains such as directly linked aromatic groups and ladder-type PDAs [14, 15]. Herein, the introduction of azobenzene groups into the side chain of PDA was expected to enhance the effective third-order NLO susceptibility Re $\chi^{(3)}$ of the PDA system.

It is worth nothing that metal and semi-conductor fine nanoparticles exhibited the enhancement of NLO properties induced by the quantum confinement effect [16]. The large picosecond optical nonlinear response of Au and Ag colloids surrounded by water or glass was firstly reported by Richard et al. [17]. Now, characteristic interactions between excitons and plasmons and their resonance effect in the hybridized systems between organic microcrystals and inorganic fine nanoparticles would make it possible to exhibit novel optical properties. As predicted theoretically [18, 19], the NLO property would be enhanced in organic microcrys-

X. Chen · G. Zou (✉) · Q. Zhang
CAS Key Laboratory of Soft Matter Chemistry, Department of Polymer Science and Engineering, Key Laboratory of Optoelectronic Science and Technology in Anhui Province, University of Science and Technology of China, Hefei, Anhui 230026, China
e-mail: gangzou@ustc.edu.cn

J. Tao · P. Wang
Department of Physics, University of Science and Technology of China, Hefei, Anhui 230026, China

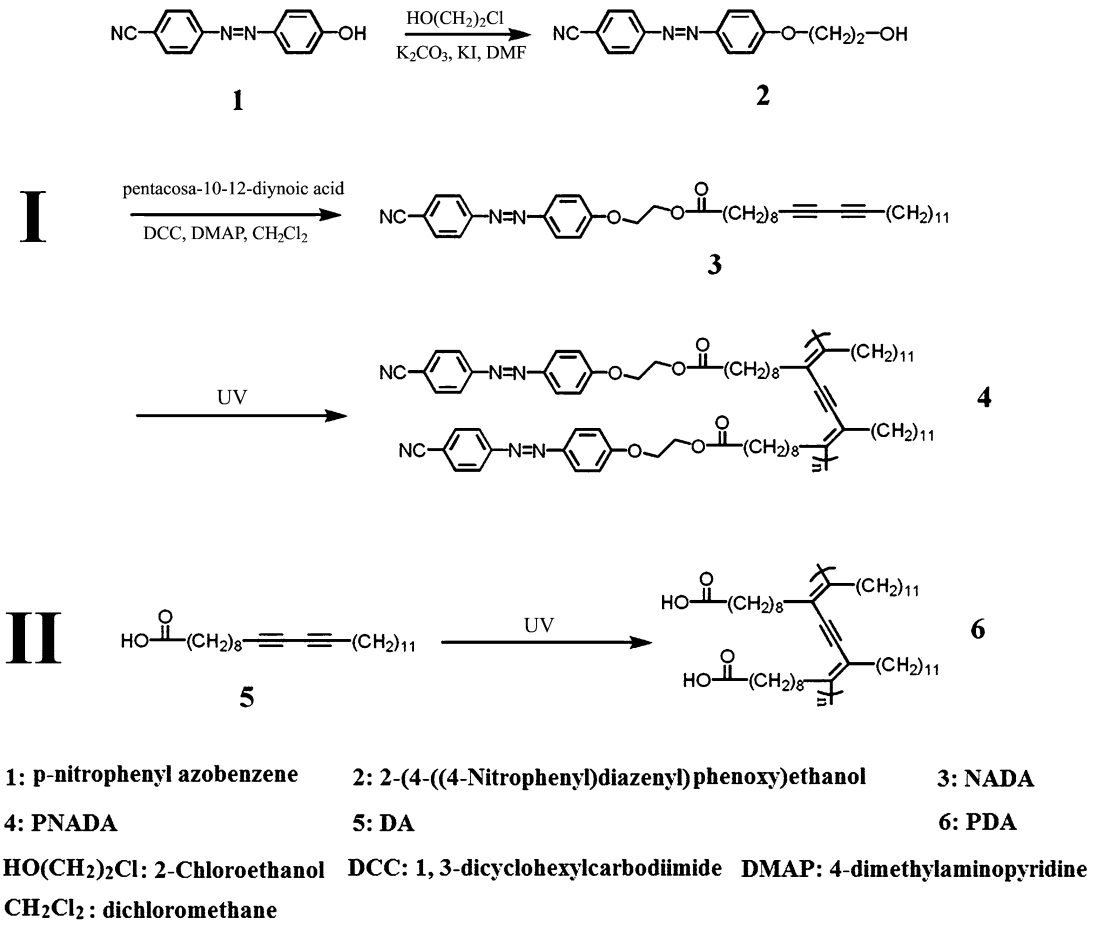

Scheme 1 Molecular structures of NADA, DA, PDA and PNADA and the synthetic routes of NADA monomer

tals coated with thin metal layers. For example, the NLO property of a PDA thin film, in which fine gold particles were dispersed, was enhanced by approximately two hundred times [20]. According to the local field enhancement under the surface plasmon resonance condition, larger third-order nonlinearity of PDA composite films had been observed in the presence of metal or semi-conductor nanoparticles [21–24]. Herein, the introduction of azobenzene and silver nanoparticles into the PDA conjugated system was expected to result in novel linear and nonlinear optical properties for PDA systems (e.g. huge enhancement of Re $\chi^{(3)}$).

In this article, p-nitrophenyl azobenzene substituted diacetylene monomer (NADA) was synthesized and Ag nanoparticle adulterated polymerized NADA films (PNADA/Ag nanocomposite films) with different concentrations of Ag nanoparticles were prepared successfully. The effective third-order nonlinear optical properties of composite films with different volume fractions of spherical silver nanoparticles were investigated in detail by the theoretical and Z-scan methods. The strategy described in this work would be useful in the development of new PDA-based optical and NLO devices.

2 Experiments

2.1 Materials

Silver nitrate, cyclohexane, polyvinylpyrrolidone, 3-methyl-1-butanol, hydrazine hydrate and sodium lauryl sulfate (SDS) were obtained from Beijing Chemical Reagent Ltd and used without further purification. 10, 12-pentacosadiynoic acid (DA) was purchased from Tokyo Chemical Industry Co. Ltd. and purified by dissolving in cyclopentanone and filtrating to remove polymer before use. The p-nitrophenyl azobenzene moiety and the diacetylene monomer containing p-nitrophenyl azobenzene moiety (NADA) were synthesized in analogy to the previous procedure [25]. The molecular structures of NADA and DA and the synthetic routes of NADA are shown in Scheme 1.

2.2 Film preparation

Ag colloidal nanoparticles were prepared according to a similar procedure as in the literature using polyvinylpyrrolidone (PVP) as a stabilizer and hydrazine hydrate as a reducing agent [26]. Silver nitrate and polyvinylpyrrolidone

were dissolved in solvent composed by water, sodium dodecyl sulfate (SDS), 3-methyl-1-butanol and cyclohexane. Then, some hydrazine hydrate was added in the system to reduce the silver nitrate. After stirring for 90 min with the temperature of 30°C, stable orange silver nanoparticles can be gained. The silver nanoparticles were purified by ultracentrifugation separation and ethanol washing several times, and then were vacuum dried at room temperature. After these, the surface modified silver nanoparticle powder was prepared, which could be easily dispersed in organic solvents by ultrasonic treatment.

The PNADA/Ag composite films were prepared by the spin-coating method. A cyclopentanone solution (0.1 ml) containing NADA (1.0×10^{-2} M) and Ag colloidal nanoparticles (from 0 μg to 80 μg) was placed on a substrate, which was then rotated at a proper speed in order to spread the fluid by centrifugal force. Rotation was continued while the fluid spins off the edges of the substrate, until the desired thickness of the film was achieved. Then, the films were exposed to UV irradiation using a high-pressure mercury lamp for photo-polymerization of DA monomers. As reference samples, a PDA film and a PDA/p-nitrophenyl azobenzene (NAZO) mixed film were prepared similarly. As the concentration of DA molecules in the PDA films was 1.0×10^{-2} M, the concentrations of DA molecules and NAZO were both 1.0×10^{-2} M in the PDA/NAZO mixed films.

2.3 Characterization

Transmission electron microscopy (TEM) and high resolution transmission electron microscopy (HRTEM) images were recorded on a Jeol-2000 microscope operated at 200 kV. For the observation, samples were obtained by dropping 5 μl of solution onto carbon-coated copper grids. All the TEM images were visualized without staining. The ultraviolet–visible (UV–vis) spectra were measured using a Shimadzu UV-2550 PC spectrophotometer (solutions were measured in a 2-mm-thick quartz cell). The thicknesses and linear refractive indices of the polymer films were measured by an ellipsometer (ELLIP-SR). The nonlinear optical properties were investigated by the Z-scan technique, using 16-ns pulse duration and 10-Hz repetition rate at 532 nm, available from a frequency-doubled Q-switched Nd:YAG laser (Quantum YG 980). The samples moved in the direction of the incident beam close to the focus of the lens, which had a focal length of 20 cm. The transmitted beam energy, the reference beam energy and their ratio were monitored by joule meters (EPM 2000), simultaneously. Z-scan measurement on CS_2 was performed to testify the stability of the system, and the obtained nonlinear refraction accords with the published result [27].

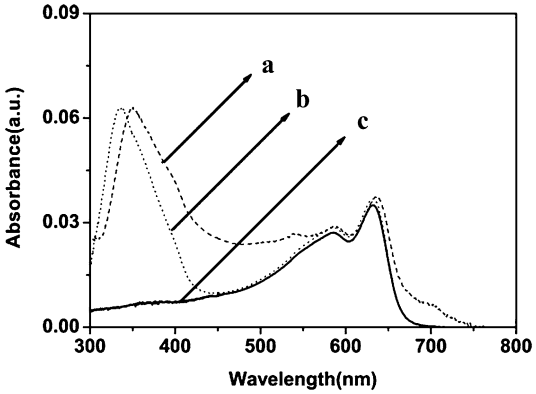

Figure 1 The optical absorption spectra of **a** (*dash*) PDA/NAZO mixed film, **b** (*dot*) PNADA film and **c** (*solid*) PDA film

3 Results and discussion

3.1 Characterization of PNADA/Ag composite films

The UV–vis absorption spectra of PNADA film, PDA film and PDA/NAZO mixed film are shown in Fig. 1. The absorption peaks at 630 and 580 nm were ascribed to the typical absorption band of the polydiacetylene chain. The absorption peaks at 350 nm and 335 nm were attributed to the π–π^* electronic transition of the azobenzene group in PNADA films and PDA/NAZO mixed films, respectively. The difference in absorption peak positions should be primarily attributed to the different molecular structure and aggregation state of the azobenzene moiety in PNADA films and PDA/NAZO mixed films. In the mixed films, the azobenzene moieties used could easily form strong H aggregation and cause the big blue shift of the absorption band (from 370 to 335 nm). For the NADA molecule, the long alkyl chain prevented the extreme accumulation of NADA in the films and only caused a slight blue shift of the absorption band (from 369 to 350 nm). Thus, the absorption peak positions for the π–π^* electronic transition of the azobenzene moiety in the mixed films and the PNADA films were different. Figure 2 illustrates the UV–vis absorption spectra of different types of the PNADA/Ag films. It is obvious that there is an isosbestic point at 350 nm in Fig. 2, which could be attributed to the π–π^* electronic transition of the same proportion of the azobenzene group in the PNADA films. Since the proportions of azobenzene groups in different types of the PNADA/Ag films were the same, the absorption peak intensity at 350 nm should be almost equal, and an isosbestic point at 350 nm appeared. The absorption peak located at 400 nm, which is known as the surface plasmon resonance oscillation of the free electrons in silver nanoparticles, increased with the increasing amount of silver nanoparticles. The linear absorption properties proved that silver nanoparticles were successfully doped in the PNADA matrix well, which is consistent with the result of TEM.

The microstructures of silver nanoparticles dispersed in the films were investigated by TEM and HRTEM. As shown in Fig. 3a, silver nanoparticles were spherical and the average size was about 10 nm. The HRTEM images testified that it was not a perfect silver crystalline layer film, and the plane distance was about 5 Å (as shown in Fig. 3b). All the above results indicate that the pure PDA films, PDA/NAZO mixed films, PNADA films and PNADA films doped with Ag nanoparticles had been fabricated successfully.

3.2 NLO characterization of PNADA/Ag composite films

NLO properties of all the above films were evaluated by means of a Z-scan technique. Open and closed aperture Z-scan measurements were used to evaluate the nonlinear refraction and nonlinear absorption properties. The nonlinear refractive index n_2 and the nonlinear absorption coefficient β were measured according to the following equations [28]:

$$n_2 = \gamma = \frac{\Delta T_{\text{p-v}}}{kI_0 L_{\text{eff}} 0.406(1-S)^{0.25}}, \tag{1}$$

$$T(z, S=1) = 1 - \frac{\beta I_0 L_{\text{eff}}}{2\sqrt{2}(1+(z/z_0)^2)}, \tag{2}$$

where $\Delta T_{\text{p-v}}$ is the difference between the normalized peak and valley transmittances: $T_{\text{p}} - T_{\text{v}}$, $k = 2\pi/\lambda$ is the wave vector, I_0 is the on-axis irradiation of the laser beam at focus ($z = 0$), $L_{\text{eff}} = (1 - \exp(-\alpha L))/\alpha$ is the effective thickness with the sample thickness L, S is the linear transmittance of the aperture, α is the linear absorption coefficient, z is the position of the sample and $z_0 = k\omega_0^2/2$ is the diffraction length of the beam. β (expressed in m/W) is correlated to the imaginary part of $\chi^{(3)}$ ($\text{Im}\,\chi^{(3)}$ expressed in esu) through [28]

$$\text{Im}\,\chi^{(3)} = \frac{9.92 \times 10^{-4} n_0^2 c\lambda}{\pi^2}\beta, \tag{3}$$

where n_0 is the linear refractive index of the sample, λ is the laser wavelength and c is the velocity of light. First, we investigated n_2 and the resulting $\text{Re}\,\chi^{(3)}$ for PNADA films, PDA films and PDA/NAZO mixed films (as shown in Fig. 4). The peak–valley configuration indicates that the nonlinear refraction was positive and thus manifests a self-focalizing effect. The nonlinear refractive index for PNADA films, PDA films and PDA/NAZO mixed films were measured to be 8.48×10^{-15} cm^2/W, 5.95×10^{-15} cm^2/W and 7.76×10^{-15} m/W, respectively. And, the resulting $\text{Re}\,\chi^{(3)}$ were calculated to be 6.08×10^{-9} esu, 4.27×10^{-9} esu and 5.56×10^{-9} esu, respectively. All the values of n_2, $\text{Re}\,\chi^{(3)}$ and $\text{Im}\,\chi^{(3)}$ for different samples are listed in Table 1. It is obvious that the nonlinearity of the PNADA films could be enhanced compared to that of pure PDA films due to the introduction of the azobenzene moiety

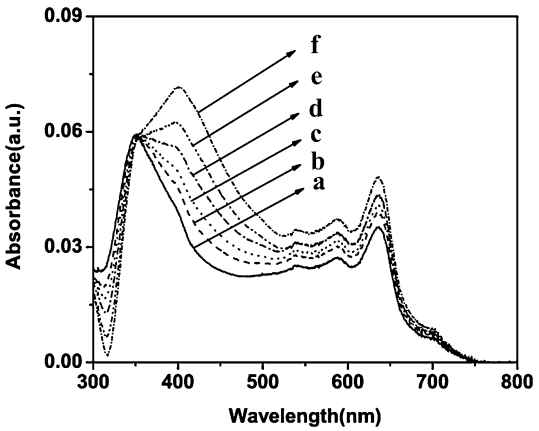

Figure 2 The optical absorption spectra of **a** (*solid*) pure PNADA film and PNADA films doped with **b** (*dash*) 20 μg, **c** (*dot*) 40 μg, **d** (*dash dot*) 60 μg, **e** (*dash dot dot*) 80 μg and **f** (*short dash dot*) 100 μg Ag nanoparticles

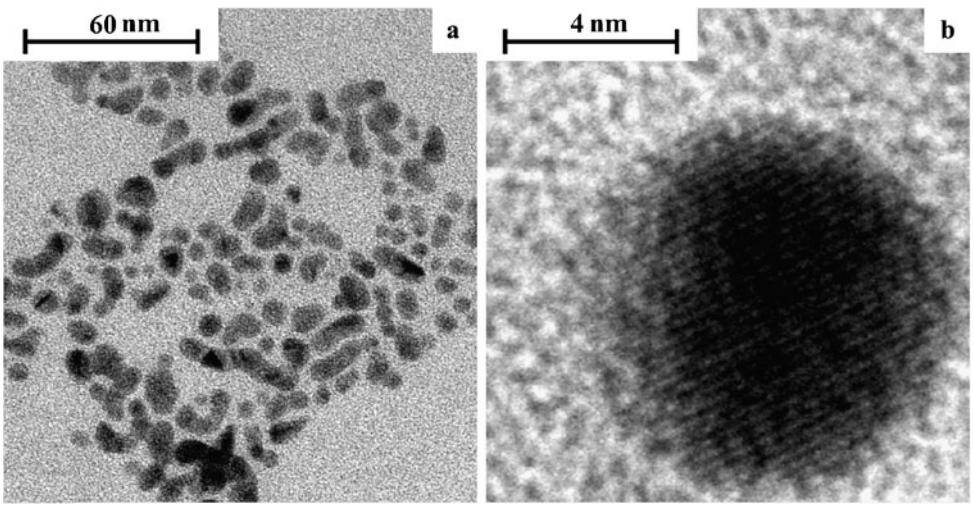

Figure 3 **a** TEM image of Ag nanoparticles (the scale bar is 60 nm) and **b** HRTEM image of Ag nanoparticles (the scale bar is 4 nm)

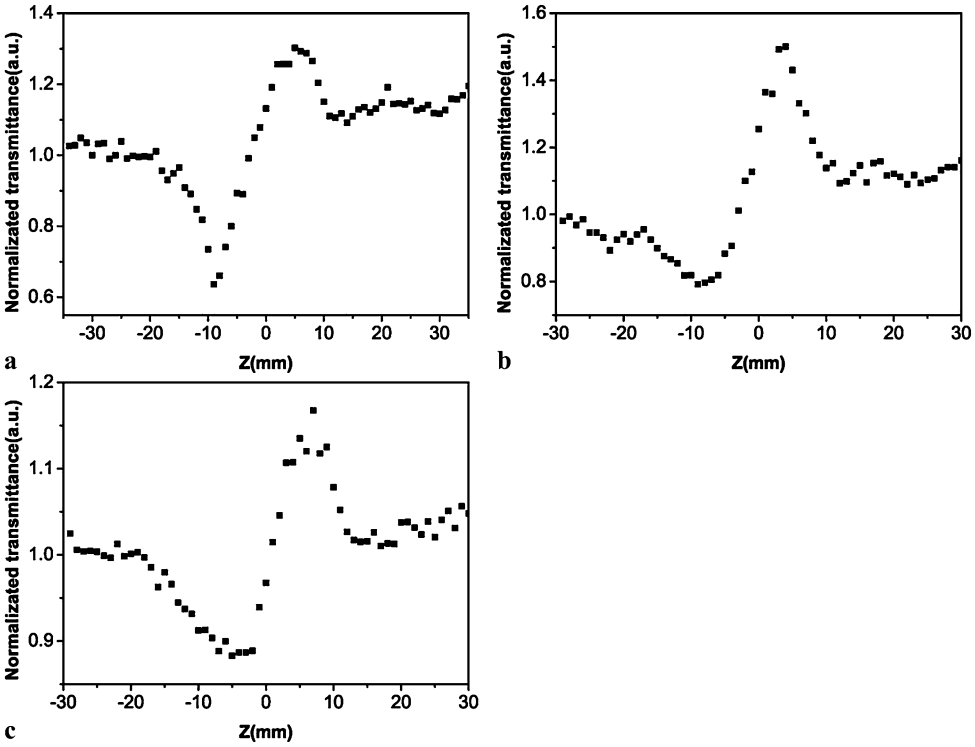

Figure 4 Measured Z-scan normalized transmittance curves of **a** pure PDA film, **b** PDA/NAZO mixed film and **c** PNADA film

Table 1 Nonlinear refractive index n_2, Re $\chi^{(3)}$ and Im $\chi^{(3)}$ for pure PDA films, PDA/NAZO mixed films, PNADA films and PNADA films doped with different volume fractions of Ag nanoparticles

Sample	Illumination	n_2 ($\times 10^{-15}$ cm^2/W)	Re $\chi^{(3)}$ ($\times 10^{-9}$ esu)	Im $\chi^{(3)}$ ($\times 10^{-8}$ esu)
Polymer films	Pure PDA film	5.9	4.2	−7.6
	PDA/NAZO mixed film	7.7	5.5	−9.8
	Pure PNADA film	8.5	6.1	−4.0
PNADA/Ag nanocomposite films	PNADA films doped with 14.5% Ag nanoparticles	9.4	6.7	−4.4
	PNADA films doped with 29% Ag nanoparticles	9.8	7.1	−5.7
	PNADA films doped with 43.5% Ag nanoparticles	11.0	7.9	−6.7
	PNADA films doped with 58% Ag nanoparticles	11.6	8.3	−10.9
	PNADA films doped with 70% Ag nanoparticles	9.5	6.8	−5.8

into the side chain and increases the electronic susceptibility. Further, we investigated n_2 and the resulting Re $\chi^{(3)}$ and Im $\chi^{(3)}$ for PNADA films doped with different concentrations of Ag nanoparticles. The nonlinear refractive indices for PNADA films doped with 0 μg, 20 μg, 40 μg, 60 μg, 80 μg and 100 μg Ag nanoparticles were measured to be 8.48×10^{-15} cm^2/W, 9.43×10^{-15} cm^2/W, 9.83×10^{-15} cm^2/W, 11×10^{-15} cm^2/W, 11.6×10^{-15} cm^2/W and 9.5×10^{-15} cm^2/W, respectively. Then, the resulting Re $\chi^{(3)}$ were calculated to be 6.08×10^{-9} esu, 6.76×10^{-9} esu, 7.05×10^{-9} esu, 7.89×10^{-9} esu, 8.32×10^{-9} esu and 6.81×10^{-9} esu, respectively. All the values of n_2, Re $\chi^{(3)}$ and Im $\chi^{(3)}$ for different samples are also listed in Table 1. The enhancement was observed to result from localized field enhancement due to the surface plasmon resonance of Ag nanoparticles in the above films. All the above results are in agreement with the theoretical prediction of Neeves and Birnboim [18] and our previous experimental results [29].

In order to describe the effect of surface concentration of silver particles more clearly, we calculated the volume fraction of silver nanoparticles according to the mass of silver nanoparticles (the method to calculate the volume fraction of Ag nanoparticles was presented in supporting information) and compared it with the simulation result. The experimental result of the third-order nonlinear optical susceptibility Re $\chi^{(3)}$ versus the volume fraction of Ag nanoparticles is shown in Fig. 5. The third-order nonlinear optical susceptibility Re $\chi^{(3)}$ increased unceasingly

when the volume fraction of silver nanoparticles changed from 0 to 58%, and the maximum appeared when the volume fraction of silver nanoparticles reached 58%. When the volume fraction of silver nanoparticles increased beyond 58%, Re $\chi^{(3)}$ was observed to decrease contrarily. Obviously, Re $\chi^{(3)}$ reached a maximum when the volume fraction of silver nanoparticles in PNADA/Ag composite films was 58%. This concentration-dependent enhancement effect of Ag colloidal nanoparticles should be attributed to the effect of localized field coupling among Ag nanoparticles. When the volume fraction of silver nanoparticles in the composite films is lower (the distance between Ag nanoparticles was great), the interaction between localized fields was relatively weak, and the electric field was mainly localized in the surface of Ag nanoparticles. With the concentration of Ag nanoparticles increasing, the distance between nanoparticles gradually decreased. When the particle distance was reduced to a certain degree, the coupling effects will markedly enhance the local field, and thus the local field was mainly distributed between the two particles. With the distance between the particles further decreasing, a particle cluster phenomenon would occur, which would reduce the local field [30]. In order to prove the above idea, TEM experiments were performed for the samples (the volume fractions of silver nanoparticles were 58% and 70%, respectively). It is obvious that the particle agglomeration could be observed when the volume fraction of silver nanoparticles reached 70%; however, the silver nanoparticles were uniform and well dispersed when the volume fraction of silver nanoparticles was 58% (as shown in Fig. 6). Thus, there is an optimum distance between the particles at which the largest local field enhancement will occur.

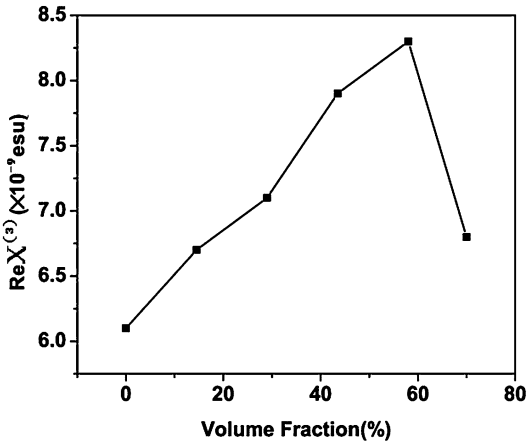

Figure 5 The variation of the third-order nonlinear optical susceptibility Re $\chi^{(3)}$ versus different volume fractions of Ag nanoparticles for PNADA/Ag composite films

The Maxwell–Garnett theory for the effective dielectric constant of a medium consisting of a collection of nanoparticles of dielectric constant ε_i immersed in a host of dielectric constant ε_h is developed in the same way as in the Clausius–Mossotti theory for the dielectric constant of a rarefied gas. Herein, the binary composite system consisting of a main matrix and metal spherical particles was taken into account. Assume that the dielectric function of the main matrix is ε_h and the linear dielectric function of the metal spherical particles is ε_i. As the metal particle size is much smaller than the incident light wavelength, in this strict quasi-static approximation the effective third-order nonlinear susceptibility can be expressed as [31]

$$\chi_e^{(3)} = P\chi_i^{(3)}\left|\frac{3\varepsilon_h}{\varepsilon_i + 2\varepsilon_h}\right|^2\left(\frac{3\varepsilon_h}{\varepsilon_i + 2\varepsilon_h}\right)^2, \tag{4}$$

where P is the volume fraction of metal particles, ε_h is the dielectric function of the main matrix, ε_i is the linear dielectric function of the spherical metal particles, $\chi_i^{(3)}$ is the third-order nonlinear susceptibility of the metal particles and $\chi_e^{(3)}$ is the effective third-order nonlinear susceptibility of the metal particle composite system. The dielectric function of silver nanoparticles at 532 nm is $\varepsilon_i = -10.073 + 0.822i$, the third-order nonlinear susceptibility of silver nanoparticles is $\chi_i^{(3)} = 8 \times 10^{-8}$ esu and the dielectric function of

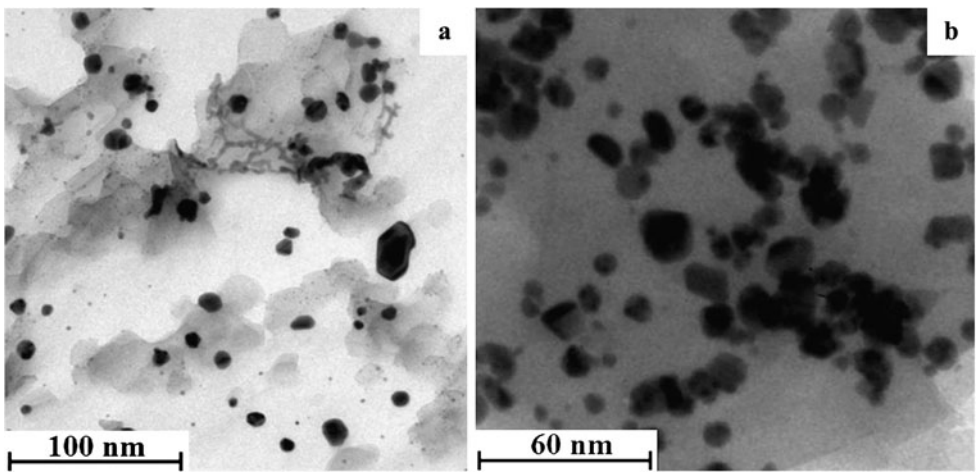

Figure 6 TEM images of PNADA/Ag composite films with the volume fractions of silver nanoparticles of **a** 58% and **b** 70%, respectively. The scale bar is 100 nm and 60 nm, respectively

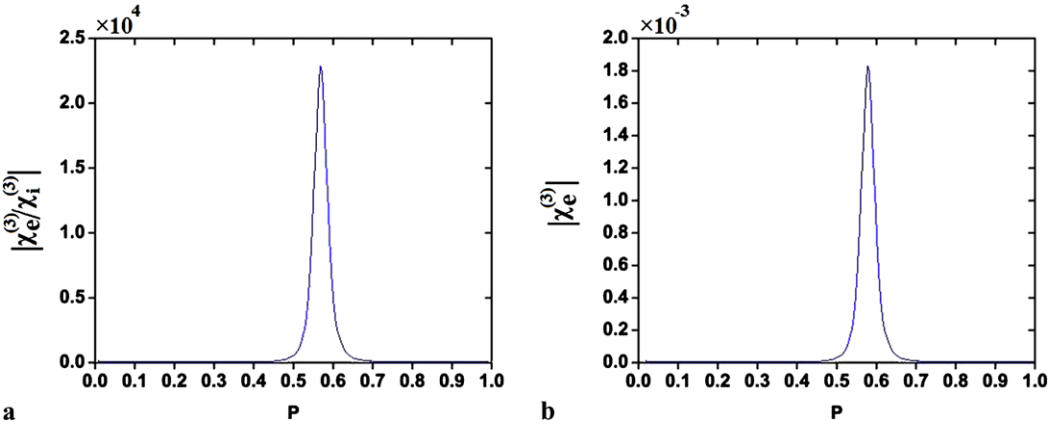

Figure 7 **a** The enhancement factor of the third-order nonlinearity ($\chi_e^{(3)}/\chi_i^{(3)}$) and **b** the third-order nonlinear optical susceptibility Re $\chi^{(3)}$ versus the volume fraction P

PDA is $\varepsilon_h = 1.3^2$. When nearing the surface plasmon resonance frequency ($\mathrm{Re}(\varepsilon_i + 2\varepsilon_h) = 0$), the effective third-order nonlinear susceptibility would be maximum. These parameters, such as the concentration of metal nanoparticles, could tune the nonlinear optical properties of the nanocomposite films.

In order to investigate the effect of the volume fraction of the metal nanoparticles on the local field and the third-order nonlinear optical properties of the films directly, we simulated the effective third-order nonlinear optical properties of composite films with different volume fractions of spherical Ag nanoparticles [32]. This concentration-dependent enhancement effect of Ag colloidal nanoparticles was validated by the Maxwell–Garnett model [33]. As shown in Fig. 7, $P = 0.58$ was the best volume fraction for the Ag nanoparticle doping, the maximum of the third-order nonlinear enhancement factor ($\chi_e^{(3)}/\chi_i^{(3)}$) was 24178 and the third-order nonlinear enhancement was 10^4 times larger than that of metal particles. All the above simulation results were almost consistent with the results of our experiment (the volume fraction of metal particles was 58% when the composite film contained 80-μg Ag nanoparticles). There is a certain value of P to keep an optimum distance between the particles at which the largest local field enhancement will occur.

4 Conclusions

In summary, pure PDA films, PDA/NAZO mixed films, PNADA films and PNADA films doped with different concentrations of Ag nanoparticles were fabricated successfully through a simple physicochemical process. The introduction of azobenzene moiety into the side chain and Ag colloidal nanoparticle doping both led to the obvious enhancement of NLO properties. The third-order nonlinear optical susceptibility Re $\chi^{(3)}$ increased unceasingly when the volume fraction of silver nanoparticles changed from 0 to 58%, and the maximum appeared when the volume fraction of silver nanoparticles reached 58%. This concentration-dependent enhancement effect of Ag nanoparticles in PNADA films was in accordance with the simulation results. The nonlinear properties of these PNADA/Ag nanocomposite films can be easily modulated by varying the concentration of Ag nanoparticles and the strategy described in this work would be useful in the development of PNADA-based optical and NLO devices.

Acknowledgements Support from the National Natural Science Foundation of China (Nos. 50703038, 50973101, 50573071, 50773035, and 50533040) and the Specialized Research Fund for the Doctoral Program of Higher Education (No. 20070358065) is gratefully acknowledged.

References

1. Ch. Bosshard, K. Sutter, Ph. Prêtre, J. Hulliger, M. Flörsheimer, P. Kaatz, P. Günter, in *Advances in Nonlinear Optics*, ed. by F. Kajzar, A.F. Garito. Organic Nonlinear Optical Materials, vol. 1 (Gordon and Breach, Basel, 1995), p. 89. Chap. 6
2. A. Sarkar, S. Okada, H. Matsuzawa, H. Matsuda, H. Nakanishi, J. Mater. Chem. **10**, 819 (2000)
3. K.D. Singer, J.E. Sohn, L.A. King et al., J. Opt. Soc. Am. B **6**(7), 1339 (1989)
4. M. Shiro, K. Kenichi, K. Takashi et al., Appl. Phys. Lett **51**(1), 1 (1987)
5. Y. Shuto, M. Amano, T. Kaino, J. Appl. Phys. **30**(2), 320 (1991)
6. Y.-S. Cho, J.-S. Lee, G. Cho, T. Wada, H. Sasabe, Polymer **42**, 9379 (2001)
7. C. Mai, Y. Lu-Ping, L.R. Dalton, Macromolecules **24**, 5421 (1991)
8. H. Nakanishi, H. Katagi, Supramol. Sci. **5**, 289 (1998)
9. S. Ohnishi, Y. Orimoto, F.L. Gu, Y. Aoki, J. Chem. Phys. **127**, 084702 (2007)
10. B. Champagne, B. Kirtman, *Handbook of Advanced Electronic and Photonic Materials and Devices* (Academic Press, New York, 2001)

11. M.Y. Balakina, J. Li, V.M. Geskin, S.R. Marder, J.L. Brêdas, J. Chem. Phys. **113**, 9598 (2000)
12. V.M. Geskin, J.L. Brêdas, J. Chem. Phys. **109**, 6163 (1998)
13. S.A. Hambir, D. Wolfe, G.J. Blanchard, G.L. Baker, J. Am. Chem. Soc. **119**, 7367 (1997)
14. F. D'Amore, A. Zappettini, G. Facchini, S.M. Pietralunga, M. Martinelli, C. Dell'Erba, C. Cuniberti, D. Comoretto, G. Dellepiane, Synth. Met. **127**, 143 (2002)
15. E. Giorgetti, G. Toci, M. Vannini, F. Giammanco, Opt. Commun. **217**(1–6), 431 (2003)
16. A.I. Ekimov, A.L. Efros, Sov. Phys. Semicond. **16**(7), 775 (1982)
17. D. Richard, P. Roussignol, C. Flytzanis, Opt. Lett. **10**, 51 (1985)
18. A.E. Neeves, M.H. Birnboim, J. Opt. Soc. Am. B **6**, 787 (1989)
19. J.W. Haus, H.S. Zhou, S. Takami, M. Hirasawa, I. Homma, H. Komiya, J. Appl. Phys. **73**(3), 1043 (1993)
20. A.W. Olsen, Z.H. Kafafi, J. Am. Chem. Soc. **113**, 7758 (1991)
21. A. Masuhara, H. Kasai, T. Kato, S. Okada, H. Oikawa, Y. Nozue, S.K. Tripathy, H. Nakanishi, J. Macromol. Sci. Pure Appl. Chem. **38**, 1371 (2001)
22. R.E. Schwerzel, K.B. Spahr, J.P. Kurmer, V.E. Wood, J.A. Jenkins, J. Phys. Chem. A **102**, 5622 (1998)
23. E. Giorgetti, G. Margheri, S. Sottini, M. Muniz-Miranda, Synth. Met. **139**, 929 (2003)
24. E. Shirai, Y. Urai, K. Itoh, J. Phys. Chem. B **102**, 3765 (1998)
25. Q. Ye, X. You, G. Zou, X.W. Yu, Q.J. Zhang, J. Mater. Chem. **18**, 2775 (2008)
26. C.M. Fiona, A.K. Nicholas, H.F. Janas, J. Chem. Soc. Faraday Trans. **91**(4), 673 (1905)
27. E. Cattaruzza, G. Battaglin, F. Gonella, G. Mattei, P. Mazzoldi, R. Polloni, B.F. Scremin, Appl. Surf. Sci **247**, 390 (2005)
28. M. Sheik-Bahae, A.A. Said, T.H. Wei, D.J. Hagan, E.W. Van Stryland, J. Quantum Electron. **26**, 760 (1990)
29. X. Chen, G. Zou, Y. Deng, Q.J. Zhang, Nanotechnology **19**, 195703 (2008)
30. Y. Hamanaka, K. Fukuta, A. Nakamura, Appl. Phys. Lett. **84**, 4938 (2004)
31. A.I. Ryasnyanskiy, B. Palpant, S. Debrus, U. Pal, A. Stepanov, J. Luminesc. **127**, 181 (2007)
32. Y. Deng, P. Wang, D.G. Zhang, L. Tang, X.J. Jian, H. Ming, Chin. J. Quantum Electron. **23**, 5 (2006)
33. G. Piredda, D.D. Smith, B. Wendling, R.W. Boyd, J. Opt. Soc. Am. B **25**, 6 (2008)